# Theoretical Limits of Hydrogen Storage in Metal−Organic Frameworks: Opportunities and Trade-Offs

Jacob Goldsmith,[†] Antek G. Wong-Foy,[‡] Michael J. Cafarella,[§] and Donald J. Siegel*,[†,⊥]

[†]Mechanical Engineering Department, [‡]Department of Chemistry, [§]Computer Science and Engineering, and [⊥]Applied Physics Program, University of Michigan, Ann Arbor, Michigan, 48109, United States

**S** *Supporting Information*

**ABSTRACT:** Because of their high surface areas, crystallinity, and tunable properties, metal−organic frameworks (MOFs) have attracted intense interest as next-generation materials for gas capture and storage. While much effort has been devoted to the discovery of new MOFs, a vast catalog of existing MOFs resides within the Cambridge Structural Database (CSD), many of whose gas uptake properties have not been assessed. Here we employ data mining and automated structure analysis to identify, "cleanup," and rapidly predict the hydrogen storage properties of these compounds. Approximately 20 000 candidate compounds were generated from the CSD using an algorithm that removes solvent/guest molecules. These compounds were then characterized with respect to their surface area and porosity. Employing the empirical relationship between excess $H_2$ uptake and surface area, we predict the theoretical total hydrogen storage capacity for the subset of ~4000 compounds exhibiting nontrivial internal porosity. Our screening identifies several overlooked compounds having high theoretical capacities; these compounds are suggested as targets of opportunity for additional experimental characterization. More importantly, screening reveals that the relationship between gravimetric and volumetric $H_2$ density is concave downward, with maximal volumetric performance occurring for surface areas of 3100−4800 $m^2$/g. We conclude that $H_2$ storage in MOFs will not benefit from further improvements in surface area alone. Rather, discovery efforts should aim to achieve moderate mass densities and surface areas simultaneously, while ensuring framework stability upon solvent removal.

**KEYWORDS:** *hydrogen storage, metal organic framework, data mining, computational screening, gas capture and storage*
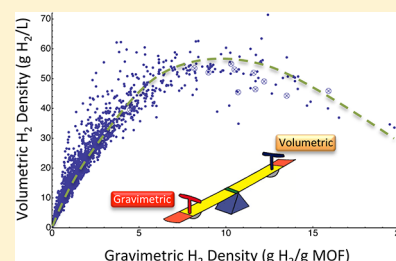
## 1. INTRODUCTION

Increasing emphasis on the development of sustainable transportation technologies has highlighted the need for high-density energy storage.[1] In the case of fuel cell vehicles (FCV), the energy storage problem can be traced to challenges associated with storing low-density gaseous $H_2$.[2] Although several approaches to storing hydrogen have been explored, (including, for example, liquefaction, physical compression, absorption in condensed phases, etc.), one of the more appealing options is the reversible adsorption of $H_2$ on high surface area materials.[2] Sorbents generally exhibit high cycle life and fast kinetics, yet are restricted to low operating temperatures due to weak $H_2$/sorbent interactions. In addition, the high gravimetric capacities typical of some sorbents rarely coincide with high volumetric densities. Consequently, the search for sorbent materials that overcome these deficiencies has emerged an extremely active area of research. In particular, the class of materials known as coordination polymers (CPs), of which a subset are termed metal−organic frameworks (MOFs), has recently attracted intense interest as hydrogen storage materials.[3−5]

MOFs are crystalline materials containing a metal atom or metal cluster bonded to organic linkers.[6−9] Thanks to their record setting surface areas, gas selectivity, and permanent, open pore geometries, MOFs have emerged as promising materials for gas storage and separations,[10] as well as for other applications.[11] MOFs are highly tunable in both structure and composition, as both metal clusters[12,13] and linkers have the potential to be varied among several possibilities. In principle, such tunability could enable the development of an adsorbent capable of storing $H_2$ at near ambient conditions and with high gravimetric and volumetric densities. Nevertheless, the extreme flexibility in MOF design also presents challenges: while a large variety of compounds are possible,[14,15] the synthesis and testing of significant numbers of compounds can be time-consuming and costly. To further complicate matters, existing materials databases (such as the Cambridge Structural Database[16]) generally do not distinguish CPs or MOFs from the large and growing number of molecular compounds.

In recognition of the bottlenecks associated with experimental materials discovery, a small number of studies have employed computational methods to rapidly characterize[17,18] or screen for promising porous materials.[15,19−22] For example, recent work[15] has screened 137 953 hypothetical MOFs for $CH_4$ uptake[15,21,22] and $CO_2$ capture[20] by interchanging 3 metals (comprising 5 metal centers) and 102 carboxylic acid derived ligands. In related work, smaller databases of MOFs were screened for use in gas separation applications.[21,22]

In the present study, we significantly expand the space of screened compounds by exploiting the 550,000+ known organic compounds contained within the Cambridge Structural Database (CSD).[16] The CSD contains thousands of MOFs,[14] yet it appears that many of these have not been tested for gas storage applications. An advantage of this approach is that it relies on existing compounds rather than on hypothetical materials that may prove difficult to synthesize. (Nevertheless, as we describe below, achieving high hydrogen capacities in known compounds still requires the synthesis of stable, solvent-free versions of these materials, a feat which is not always straightforward.) To facilitate a computational assessment of these properties, we use data mining and structural routines to identify, "cleanup," and rapidly characterize MOFs within the CSD. The isolation of such structures enables rapid prediction of their performance and allows us to address fundamental questions regarding their properties. For example: Which MOFs have the highest theoretical $H_2$ capacity, and what common features do they share? Can high surface and high volumetric density of stored $H_2$ be achieved simultaneously? Answering these questions will accelerate the discovery of optimal MOFs for hydrogen storage applications.

Here we demonstrate such an approach by searching for MOFs exhibiting high hydrogen storage capacities.[2] A subset of ~22 700 compounds is generated from the CSD using search and filtering algorithms, followed by routines for the removal of guest molecules or fragments thereof. The resulting structures are characterized with respect to their surface area[23] and pore volume. Application of the empirical correlation between $H_2$ excess uptake and surface area allows for the theoretical total hydrogen storage capacity to be estimated for the subset of ~4000 compounds exhibiting nontrivial internal porosity. This approach is relatively efficient as it does not require the evaluation of interatomic potentials or expensive isotherm simulations — only geometric features of the crystal structure need to be assessed. Moreover, by comparing theoretical capacities we avoid experimental complications associated with incomplete solvent removal; this allows for consistent comparisons across compounds and analysis of trade-offs and trends that could be difficult to isolate using (potentially noisy) experimental data.

Our screening identifies several known, yet overlooked compounds having high hydrogen storage densities exceeding 10 wt % (g $H_2$/g MOF basis) and 58 g/L (total $H_2$, at 77K and 35 bar). These compounds are suggested as promising candidates worthy of additional experimental characterization. More importantly, screening also reveals a maximum in the distribution of volumetric vs gravimetric uptake data, beyond which additional increases in surface area result in decreasing volumetric capacity. Such a trade-off implies that $H_2$ storage in MOFs will not benefit from further improvements in surface area alone. Rather, materials development efforts should aim to simultaneously achieve moderate mass densities and surface areas, while ensuring framework rubustness upon solvent removal.

## 2. METHODOLOGY

**2.1. Structure Searching.** A flow diagram summarizing the key steps in our MOF screening scheme is given in Figure 1. As a first step, MOF crystal structures were identified and extracted from the CSD. The CSD is a database containing more than 600K crystal structures, 550K of which are distinct organic compounds (top box in Figure 1). Because the rate of structural depositions in the CSD doubles roughly
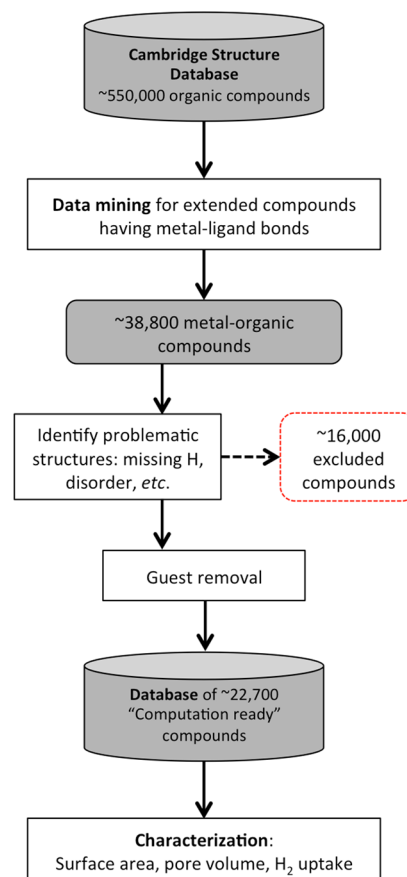


**Figure 1.** Flow diagram summarizing the processing and analysis of crystal structure data from the CSD.

every 9 years,[14] and doubles approximately every 4 years for MOFs,[14] we sought to develop methods to identify MOFs which could be reused upon subsequent updates to the CSD. To facilitate structure analysis, all compounds of interest were translated from the native crystallographic information file (CIF) format of the CSD to explicit *xyz* atomic coordinates using the Atomic Simulation Environment (ASE),[24] a Python code for structural analysis.

A labeled data set of previously identified MOFs[14] (2nd box in Figure 1) was employed to verify data features that indicate MOFs. By using these features we were able to identify MOFs in the labeled set with >95% recall. That is, had we known these features beforehand and searched the labeled data set, we would have found >95% of the structures. Those features were: structures that contain carbon, a metal, a ligand, and a metal−ligand bond; and structures labeled as an extended structure. For this search, we defined a metal to include all metals to the right of the diagonal along (Al to Po), the f-block metals, but not the alkali metals. Ligands are defined as elements that can form bonds between metal and organic components, and we included the elements B, N, O, Si, P, and S in our search.

To identify the presence of a metal−ligand bond we evaluated pair distances between each atom within the crystallographic unit cell. To determine whether a given pair of atoms $i$ and $j$ are bonded we compare their geometric distance ($d_{ij}$) to a set of known atomic bond radii ($r$). These radii are computed averages from the CSD and required use of a broadening term $\sigma = 0.5$ Å, to take into account bond length variation: $d_{ij} < r_i + r_j + \sigma$. Our initial search implementing these criteria identified approximately 38 800 metal−organic compounds, Figure 1.

Our analysis of the data contained within the CSD revealed several examples of structural irregularities. These include missing hydrogen, missing atom coordinates (i.e., fractional coordinates labeled with a '?'), ionic species, and partial site occupancies arising from high symmetry conformations. (Because in the latter case the CSD does not

generally provide site occupancies, we found that atomic coordinates that are too close to be physically bonded (<0.7 A) often served as a good indicator of symmetry-related disorder.) We observe that disorder is often present in structures having large unit cells or thermal conformational degrees of freedom, both traits common to MOFs. Missing atoms are often solvent or hydrogen. Compounds containing ionic species were also excluded from the database to avoid charge imbalance; these ionic species often appear in conjunction with guest molecules that are later removed (see section 2.2). Because our procedure examines more files than a human can realistically process, automated identification and isolation of potentially troublesome structures was necessary. Scanning for these problematic features resulted in the identification and isolation (i.e., removal) of ~16K compounds (see red box in Figure 1).

**2.2. Guest Removal.** The next step in our processing involved the removal of unbounded guest molecules from the remaining structures. Guests typically consist of residual solvent incorporated into the MOF pores during crystallization. To maximize porosity and surface area, it is desirable to remove guests from the structure, for example, by evacuation and heating. In some cases, guest removal is not complete; hence, the crystal structure data within the CSD can contain (partially resolved) positions of solvent atoms. As our goal is to estimate the maximum theoretical capacity of MOFs for $H_2$ storage, we developed an algorithm to remove these guests and thereby create pristine (i.e., solvent free) MOFs.

Our guest removal algorithm operates by constructing a molecular graph of the structure by processing the distances $d_{ij}$ between each pair of atoms, then expanding the connectivity to a periodic cell. In this way the connectivity of the metal organic framework and all other bonded components were identified. We postulated that the set of bonded atoms could be split into two distinct sets, one containing the metal−organic framework and the other containing all other components. Those components not part of the metal's bonded network are presumed to be guest molecules and are removed.

For gas storage applications it is desirable that the adsorbent material consist of a semirigid, 3D periodic framework of covalently bonded atoms. However, less interesting compounds consisting of 1D or 2D building blocks that are held together by hydrogen bond networks or van der Waals forces can also appear in the data set. These compounds contain multiple connected components lists containing metals, and may complicate the guest removal algorithm. To filter out the 1D and 2D compounds, we reasoned that a 3D framework should have a single connected component list containing all metals in the unit cell. To test this hypothesis, we applied this assumption to our labeled set, and found it true for >95% of the set cases. (Of course, interpenetrated MOFs can have multiple metal lists, and one disadvantage of this approach is that it excludes these compounds from our data set.) We found that so long as the structure was an extended 3D MOF, our method removed solvents and guests correctly. As a further check on the method's accuracy, we examined the most promising MOF structures by hand to ensure these were free of errors. An example of successful guest removal is shown in Figure 2, where the guests are comprised of water molecules. More generally, we observe that structures whose authors used the PLATON SQUEEZE[25] function to refine their structures before submission to the CSD typically produced a crystal structure free from guest molecules. The final step in cleaning up the structures involved removing terminal oxygen atoms bonded to metal sites. These atoms appear to be components of incompletely resolved water molecules that are missing H atoms.

**2.3. Surface Area, Porosity, and Theoretical $H_2$ Uptake.** With the removal of unbounded guests we have amassed a database of approximately 22,700 "computation ready" compounds amenable to property characterization (Figure 1). For gas storage applications, two key properties of an adsorbent are surface area and porosity. Surface area is significant because it relates to the number of possible sites at which adsorption can take place. In fact, the excess gravimetric uptake arising from adsorption correlates strongly with surface area in a wide range of porous materials.[26] Likewise, porosity determines the amount of free space available to host gas phase (or "bulk") molecules of the

0 m²/g    567 m²/g
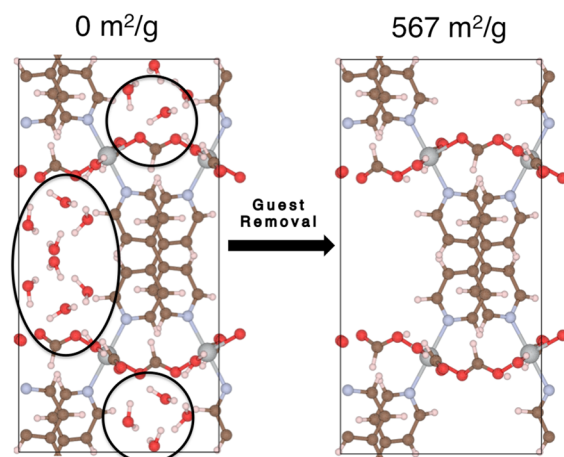


**Figure 2.** Example of the automated removal of guest molecules from the compound FIFPAM, and the resulting increase in surface area. The circles indicate unconnected components (water molecules) in the MOF's molecular graph.

adsorbate. By combining the adsorbed and bulk quantities of adsorbate one can estimate the total amount of a gas stored within a given adsorbent. Thus as a next step we calculate the surface areas and porosities for all compounds in our database.

For surface area calculations we adopt the geometric accessible surface area approach described in ref 23. The method was validated by comparing calculated surface areas from the data set compounds against previous applications of the method.[23] Following convention, we use a probe of $N_2$ of 3.681 Å diameter; unit-cell lattice parameters were read from the CIF file without further modification. Figure 2 demonstrates how the calculated surface area increases after the removal of guest molecules. To calculate the porosity we used the CALC SOLV function within the PLATON code[25] and a $H_2$ probe molecule.

In previous work on $H_2$ adsorption in microporous carbons, a linear relationship (i.e., the so-called "Chahine rule")[26] was observed between surface area and excess hydrogen uptake, $n_{excess}$, at 77 K and 35 bar. Upon further investigation, this relationship was found to hold across a wide class of porous materials, including MOFs.[27,28] It is possible to estimate the total amount of $H_2$ stored by a given MOF by augmenting $n_{excess}$ with $n_{gas}$, the amount of gas phase hydrogen present in the MOF's pore, $n_{gas} = \rho_{H_2} V_{pore}$. Here $\rho_{H_2}$ is the density of hydrogen at 77 K and 35 bar (11.5 kg/m³), and $V_{pore}$ is the volume within the pores of the crystallographic unit cell as calculated by PLATON. The total uptake can be described by the following equation

$$n_{tot} = n_{excess} + n_{gas} = C \cdot SA + \rho_{H_2} V_{pore} \tag{1}$$

where $C$ is the proportionality constant (0.021 mg $H_2$/m²) linking surface area (SA) with excess uptake.[28] We note that this proportionality constant is valid only for a specific temperature and pressure, in this case 77 K and 35 bar. Dividing $n_{tot}$ by the mass or volume of the unit cell yields, respectively, the total gravimetric (units of g $H_2$ per g MOF) and total volumetric uptake (units of g $H_2$ per L of MOF) of $H_2$.

We emphasize that our estimate of total $H_2$ uptake refers to the maximum theoretical uptake on a materials basis. That is, we assume a pristine MOF in which all solvent molecules have been removed, and furthermore take $V_{pore}$ to be the micropore volume within a single-crystal monolith of the MOF. (In other words, the theoretical volumetric density of stored $H_2$ is based on the single crystal MOF density: Volumetric density = gravimetric density × single-crystal density.) Although MOF synthesis procedures are continually improving (resulting in less solvent retained within the pores),[29] and densification has shown promise for improving MOF density,[30,31] it is unlikely that MOF media used in a commercial storage system will adopt a single crystal morphology and be completely free from guest

molecules. In addition, gravimetric and volumetric losses will arise from the mass and volume associated with the storage system: e.g., pressure vessel, balance of plant components, etc. Hence, our estimates represent an upper bound to the $H_2$ storage performance. Nevertheless, such estimates are of value because they can distinguish "dead-end" materials, i.e., materials that do not at least exceed system-level targets on a materials-only basis, from those that show promise. Moreover, the use of theoretical capacities facilitates comparisons between compounds by avoiding experimental complications associated with incomplete (or inconsistent) solvent removal. This allows for the identification of trade-offs and trends that may be difficult to isolate using experimental data derived from different synthesis conditions.

## 3. RESULTS AND DISCUSSION

**3.1. Surface Area, Density, and Porosity.** After the removal of guest molecules, calculation of the surface areas for all compounds reveals that the database contains 4026 MOFs with nonzero surface areas; 568 of these exhibit moderately high surface areas >1000 $m^2/g$. A histogram illustrating the number of compounds with a given surface area is shown in Figure 3. The distribution is sharply peaked at low surface areas,
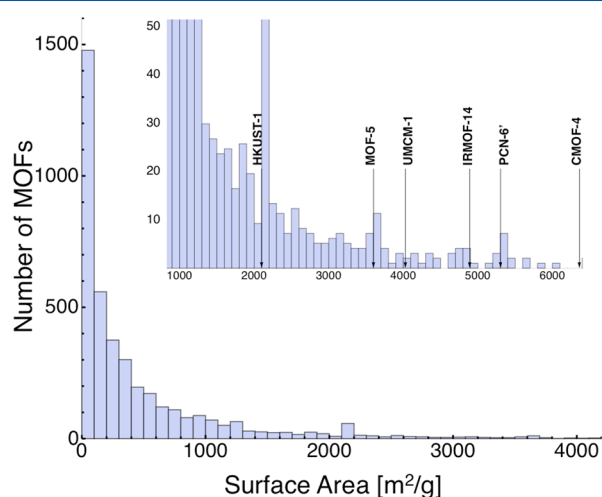


**Figure 3.** Number of MOFs having a given surface area. Labels highlight selected common MOFs. The inset magnifies the distribution for MOFs having surface area >1000 $m^2/g$. The peak in the distribution near 2100 $m^2/g$ is due to multiple entries for HKUST-1.

and exhibits a long tail out to values in excess of 5000 $m^2/g$. The presence of a small number of compounds having large surface areas is consistent with recent experimental measurements showing that a handful of compounds have surface areas in the range of 5000–6000 $m^2/g$.[3]

Because surface area directly relates to gravimetric excess uptake, and is therefore a key component in estimating total $H_2$ stored (eq 1), it is important to assess the degree to which calculated surface areas correlate with experimental measurements, the latter being most commonly based on BET theory. Since the experimental BET surface area depends on the pressure range used in its estimation, as well as on the purity and defect structure of the MOF, care should be exercised in making direct comparisons between theory an experiment; a thorough discussion of these issues is provided in ref 23. Figure 4 plots the experimental BET surface area vs. the calculated surface area for a subset of MOFs whose surface areas have been measured experimentally. The general trend in the data is
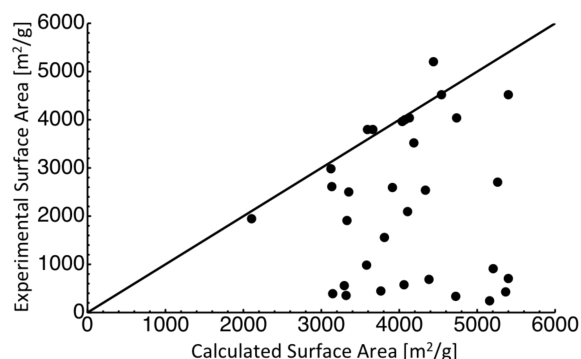


**Figure 4.** Comparison of calculated surface areas with experimentally measured surface areas for selected MOFs. The diagonal line indicates perfect agreement between theory and experiments.

for the computed surface areas to exceed the experimentally measured areas: that is, the majority of points fall on or below the diagonal line in Figure 4. The trends in Figure 4 can be explained as follows: the optimization of synthesis procedures over time has resulted in significant improvements to the surface area of MOFs, for example through more complete removal of guests or unreacted reactants.[29] Hence, those MOFs exhibiting good agreement between the calculated and measured surface area represent compositions in which essentially all solvent has been removed. On the other hand, compounds that fall below the diagonal line in Figure 4 represent cases where solvent was either not completely removed, or for which the process of solvent removal results in a change in the MOF structure, such as framework collapse. We expect that the agreement between calculated and measured surface areas will improve as synthesis procedures evolve. As an example we cite the evolving surface area of MOF-5, which is perhaps the most heavily studied MOF. Early efforts targeting the synthesis of MOF-5 did not achieve maximal surface areas. Only after an optimal procedure was identified[29] did the measured surface area (~3800 $m^2/g$) approach the theoretical value (~3656 $m^2/g$), Figure S1 in the Supporting Information. We conclude that the calculated surface area represents a reasonable upper bound to both the experimentally achievable surface area and, through the Chahine rule, the excess gravimetric density of stored $H_2$.

In addition to gravimetric density, the volumetric density of stored $H_2$ is another important, but relatively unappreciated, performance metric. Recent MOF synthesis efforts appear to focus on maximizing surface area and gravimetric performance at the possible expense of volumetric density. The product of gravimetric density and the mass density is equal to the volumetric density; and from the Chahine rule, we know that gravimetric density is proportional to surface area, eq 1. Therefore to simultaneously maximize gravimetric and volumetric performance, compounds having both high surface areas and high mass densities are needed. Do these materials exist? To answer this, Figure 5 plots the mass density vs. calculated surface area for the database MOFs. (A plot of atomic number density vs SA is given in Figure S2 in the Supporting Information.) Figure 5 shows that MOF density decreases with increasing surface area. The decrease is rapid and nonlinear for surface areas less than 1000 $m_2/g$, and then transitions to a roughly linear relation for surfaces areas in excess of 2000 $m^2/g$. The inverse relationship between SA and density indicates the potential for a trade-off between
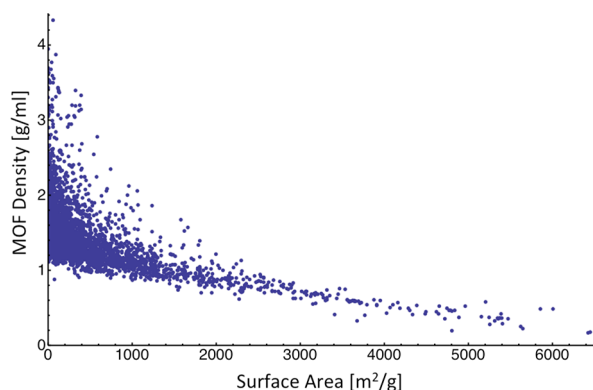
**Figure 5.** MOF mass density vs. calculated surface area.

volumetric and gravimetric H$_2$ density; this will be discussed in more detail below. Interestingly, extrapolation of the linear relationship between density and surface area results in an intercept of ~7750 m$^2$/g, corresponding to the surface area of a hypothetical MOF having a density of zero. This value is somewhat smaller than the ~10 500 m$^2$/g upper limit for a hypothetical MOF consisting of infinitely long linkers derived from benzene rings,[32] and may represent a more realistic estimate of the maximum surface area attainable by MOFs.

To estimate the total H$_2$ contained within a MOF, it is necessary to quantify the amount of pore space available for gas phase (bulk) H$_2$. Histograms of the calculated porosity and void percentage of the data set compounds are shown in Figure S3 in the Supporting Information. Similar to surface area, these distributions are peaked at moderate values for pore volume or void fraction, with very long tails extending out to higher values. The data confirm that very few compounds exhibit extremely high porosity.

**3.2. Theoretical H$_2$ Storage.** Figure 6 plots the theoretical total H$_2$ uptake (at 77 K and 35 bar) for the database compounds having nonzero surface areas. In several cases the data points corresponding to noteworthy compounds are highlighted. The calculated values are compared with the DOE 2017 hydrogen storage system targets of 5.5 wt % and 40 g H$_2$/L, depicted as the rectangular region in the upper-right corner of the plot.[2] Table 1 summarizes the properties of 78 high-performing compounds identified by screening with gravimetric capacities greater than 7.5 wt % [(g H$_2$/g MOF) × 100]. (Figure S4 in the Supporting Information contains an alternative version of Figure 6 in which gravimetric density is reported in units of g H$_2$/(g H$_2$ + g MOF) × 100.) Of these high gravimetric compounds, nearly 8% appear to be variants of MOF-5, whereas 52% contain Zn-based clusters and 28% contain Cu clusters. The limited diversity in metal content suggests that opportunities may exist to expand the composition space via metal substitution.

Several features of Figure 6 are noteworthy. First, it is clear that the vast majority of porous compounds exhibit relatively low H$_2$ uptake. Nevertheless, our screening identifies several dozen that surpass the targets on a theoretical, materials-only basis (Table 1). Second, and perhaps more importantly, the distribution of volumetric capacities exhibits a concave downward shape when plotted vs. wt %. That is, at capacities below ~5 wt % the volumetric and gravimetric densities are positively correlated. However, upon continuing to higher wt % the volumetric density approaches a maximum of ~64 g/L at
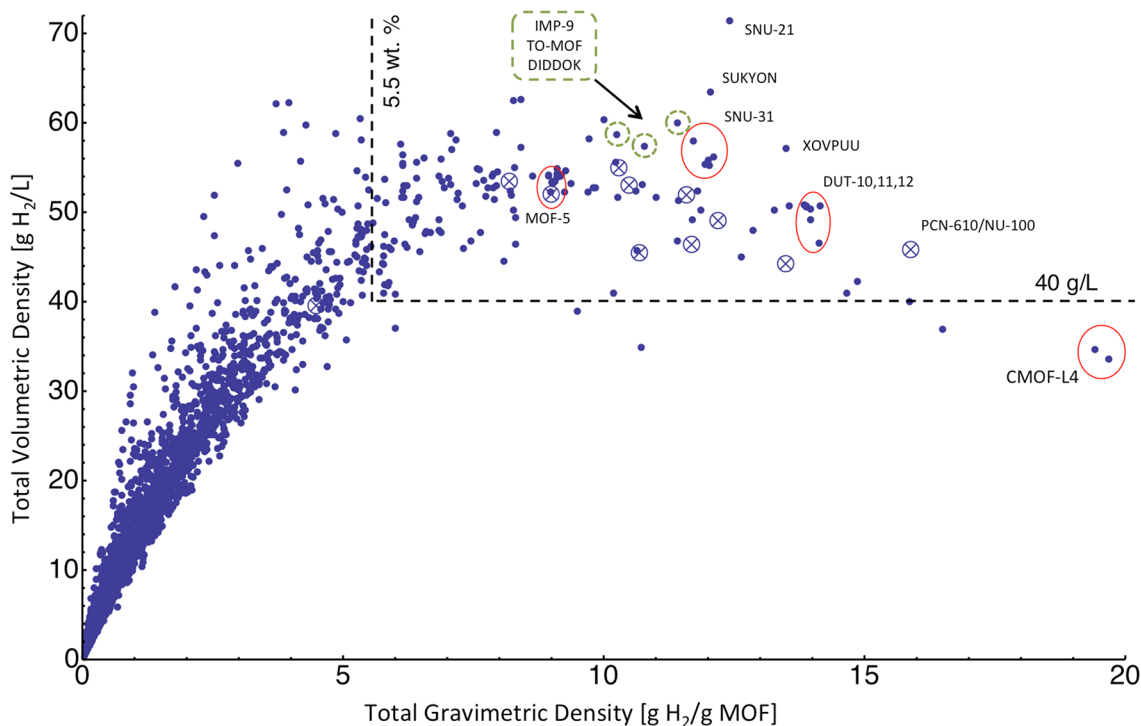


**Figure 6.** Theoretical total (adsorbed + gas phase H$_2$ at 77 K and 35 bar) volumetric and gravimetric density of stored H$_2$ in ~4000 MOFs mined from the CSD. The data account only for the mass and volume of the MOF media; mass and volume contributions from the system are neglected. For comparison, the region bounded by the dashed lines represents the DOE 2017 targets for H$_2$ storage systems. Crossed circles represent common MOFs with incomplete or disordered crystal data in the CSD; structures for these compounds were constructed by hand. Additional data for the top-performing MOFs is given in Table 1.

**Table 1. Calculated Properties of Selected Database MOFs Having Gravimetric Capacities Greater than 7.5 wt %[a]**

| CSD identifier, common name, and reference | density (g/cm$^3$) | S.A. calcd/expt (m$^2$/g) | porosity (cm$^3$/g) | calcd total grav. density (g H$_2$/g MOF) | calcd total vol. density (g H$_2$/L) | notes regarding prior experimental measurements, if available |
|---|---|---|---|---|---|---|
| | | | Compounds for Which H$_2$ Uptake Has Not Been Reported | | | |
| CMOF-L4b (XAHQAA[34]) | 0.17 | 6424 | 5.39 | 19.7 | 33.5 | pores collapse upon solvent removal |
| CMOF-L4 (XAHPUT[34]) | 0.18 | 6451 | 5.10 | 19.4 | 34.7 | pores collapse upon solvent removal |
| MOF-HTB (NIBJAK[40]) | 0.22 | 5648 | 4.04 | 16.5 | 36.9 | |
| mesoMOF-1 (HEXVEM[41]) | 0.25 | 5623 | 3.53 | 15.9 | 39.9 | |
| CMOF-L3 (XAHPON[34]) | 0.28 | 5405 | 3.05 | 14.9 | 42.2 | pores collapse upon solvent removal |
| DUT-10(Co) (XAFFIV[42]) | 0.36 | 5474 | 2.31 | 14.2 | 50.7 | likely similar uptake to DUT-10(Zn) |
| DUT-11 (XAFFER[42]) | 0.36 | 5397 | 2.30 | 14.0 | 50.3 | |
| DUT-10(Cu) (XAFFOB[42]) | 0.37 | 5350 | 2.27 | 13.8 | 50.7 | uptake likely similar to DUT-10(Zn) |
| CMOF-L2 (XAHPED[34]) | 0.37 | 5250 | 2.19 | 13.6 | 50.7 | pores collapse upon solvent removal |
| CMOF-L1b (XAHPIH[34]) | 0.36 | 4723/343 | 2.37 | 12.6 | 45.0 | pores collapse upon solvent removal |
| UMCM-151 (ANUGEW[43]) | 0.44 | 4621 | 1.82 | 11.8 | 52.3 | |
| PUZLOM[44] | 0.45 | 4494 | 1.73 | 11.4 | 51.3 | C$_{60}$ uptake measured |
| DIDDOK[37] | 0.53 | 4651 | 1.42 | 11.4 | 60.0 | |
| WAGYUA[45] | 0.47 | 4305 | 1.70 | 11.0 | 51.7 | |
| TO-MOF (LURGEL[39]) | 0.53 | 4386/680 | 1.36 | 10.8 | 57.3 | CO$_2$ uptake measured |
| ECOKAJ[46] | 0.33 | 3680 | 2.60 | 10.7 | 34.9 | |
| XUTQEI[47] | 0.49 | 4284 | 1.51 | 10.7 | 53.0 | |
| LIHFAK[48] | 0.50 | 4066/580 | 1.52 | 10.3 | 51.7 | luminescence measured |
| DUT-28 (AXINAX01[49]) | 0.40 | 3767/450 | 1.98 | 10.2 | 41.0 | |
| IMP-9 (ENITAX[38]) | 0.57 | 4162 | 1.31 | 10.2 | 58.7 | |
| UiO-68 (UVUFEX[50]) | 0.54 | 3909 | 1.42 | 9.8 | 52.7 | |
| FUNBOG[51] | 0.58 | 3583/980 | 1.28 | 9.0 | 52.3 | CO$_2$ uptake measured |
| ALUKOI[52] | 0.74 | 3531 | 0.87 | 8.4 | 62.6 | magnetic properties measured |
| WONZUV[53] | 0.61 | 3317 | 1.14 | 8.3 | 50.3 | |
| ALULAV[52] | 0.76 | 3466 | 0.86 | 8.3 | 62.5 | |
| PPF-5 (QOQBOO[54]) | 0.63 | 3274 | 1.18 | 8.2 | 52.0 | |
| XOXMED[55] | 0.55 | 3150/400 | 1.27 | 8.0 | 44.6 | |
| IRMOF-3 $\alpha$ (VURMOL[56]) | 0.69 | 3212 | 1.05 | 8.0 | 54.5 | |
| AMOFAK[57] | 0.74 | 3313 | 0.86 | 7.9 | 58.9 | luminescence measured |
| QATCUJ[58] | 0.69 | 3245 | 0.93 | 7.9 | 54.2 | |
| OKERAY[59] | 0.63 | 3005 | 1.15 | 7.6 | 47.7 | pores collapse upon solvent removal |
| | | | High-Performing Compounds for Which H$_2$ Uptake Has Been Measured | | | |
| PCN-610 or NU-100[35] | 0.29 | 5723/6143 | 3.37 | 15.9 | 46.2 | 1.82; 16.4 wt % (77 K, 1; 70 bar) |
| PCN-6′ (NIBHOW[40]) | 0.28 | 5258/2700 | 3.15 | 14.7 | 41.0 | 1.35 wt % (77 K, 1 bar) |
| DUT-12(Cu) (XAFFUH[42]) | 0.33 | 5312 | 2.58 | 14.1 | 46.5 | 1.3 wt % (77 K, 1 bar) |
| SNU-30SC (VAGMEX[60]) | 0.37 | 5416 | 2.26 | 14.0 | 51.2 | similar to SNU-30 |
| DUT-10(Zn) (XAFFAN[42]) | 0.37 | 5370/423 | 2.26 | 13.9 | 50.7 | 0.7 wt % (77 K, 1 bar) |
| SNU-30 (VAGMAT[60]) | 0.38 | 5402/704 | 2.16 | 13.8 | 52.5 | 1.42; 3.27 (77 K, 1 bar; 77 K, 62 bar) |
| IRMOF-10[61] | 0.33 | 5026 | 2.60 | 13.6 | 44.6 | 12 wt %; 43 g/L (77K, 80 bar, GCMC) |
| XOVPUU[62] | 0.42 | 5392/1217[L] | 1.90 | 13.5 | 57.1 | 1.1 wt % (77 K, 1 bar, GCMC) |
| OWIZAW[45] | 0.38 | 5155/252 | 2.12 | 13.3 | 50.2 | 1.1 wt % (77 K, 1 bar) |
| IRMOF-14 (EDUVOO[63]) | 0.37 | 4891 | 2.27 | 12.9 | 48.0 | ~1.7; ~10 wt % (77 K; 300 K, 100 bar, GCMC) |
| SNU-21(S,H) (EPOTAF[33]) | 0.58 | 5208/905 (S), 695(H) | 1.29 | 12.4 | 71.4 | 5 wt % (77K, 70 bar) |
| FJI-1[4] | 0.41 | 4731/4043 | 1.95 | 12.2 | 49.4 | 1.02; 9.08 wt % (77K, 1; 62 bar), 0.43 wt % (298 K, 65 bar) |
| XAWVUN[64] | 0.46 | 4833/626[L] | 1.71 | 12.1 | 56.2 | 1.4 wt % (77 K, 1 bar) |
| SNU-31 (VAGMIB[60]) | 0.46 | 4804 | 1.69 | 12.0 | 55.2 | 0.2 wt % (77 K, 1 bar) |
| XEBHOC[64] | 0.47 | 4784/504[L] | 1.70 | 12.0 | 55.8 | 1.2 wt % (77 K, 1 bar) |
| SNU-31 MeCN (VAGMIB01[60]) | 0.46 | 4767 | 1.67 | 11.9 | 55.3 | similar to SNU-31 |
| OHUKIM[65] | 0.42 | 4645 | 1.82 | 11.9 | 50.2 | 6.0; 9.2 (43 g/L) wt% (77 K, 20; 100 bar) |
| SNU-31SC (VAGMOH[60]) | 0.49 | 4742 | 1.53 | 11.7 | 58.0 | similar to SNU-31 |
| UMCM-2[3] | 0.40 | 4436/5200 | 2.09 | 11.7 | 46.9 | 6.9 wt % (77 K, 46 bar) |
| MOF-177 (ERIRIG)[4] | 0.45 | 4547/4750 | 1.78 | 11.6 | 52.3 | 1.25; 7 .5 wt % (77 K, 1; 90 bar) |
| DUT-13 (EHIJAH)[66] | 0.41 | 4332/2532 | 2.01 | 11.4 | 46.8 | 5.23 wt % (77K, 56 bar) |
| SUKYON[67] | 0.55 | 4577/1020 | 1.34 | 11.2 | 60.7 | 1.73 wt % (77 K, 1 bar) |
| UMCM-1[3] | 0.43 | 4041/3971 | 1.90 | 10.7 | 45.8 | 1.35 wt % (77 K, 1 bar) |

**Table 1. continued**

| CSD identifier, common name, and reference | density (g/cm³) | S.A. calcd/expt (m²/g) | porosity (cm³/g) | calcd total grav. density (g H₂/g MOF) | calcd total vol. density (g H₂/L) | notes regarding prior experimental measurements, if available |
|---|---|---|---|---|---|---|
| | | | High-Performing Compounds for Which H₂ Uptake Has Been Measured | | | |
| PCN-20 (LUKLIN)[68] | 0.49 | 4185/3525 | 1.58 | 10.6 | 52.4 | 6 wt % (77 K, 35 bar) |
| UMCM-8[69] | 0.51 | 4131/4030 | 1.55 | 10.5 | 53.5 | 1.23 wt % (77 K, 1 bar) |
| PCN-66[4] | 0.54 | 4078/4000 | 1.49 | 10.3 | 55.3 | 1.79; 6.65 wt % (77 K, 1; 45 bar), 0.78 wt % (298 K, 90 bar) |
| JEJWEB[70] | 0.54 | 4104/2095 | 1.39 | 10.2 | 55.6 | 0.8 wt % (77 K, 1 bar) |
| GAHWIX[71] | 0.60 | 3878 | 1.61 | 10.0 | 60.3 | pores collapse; no gas uptake |
| SNU-6 (ROGMEG)[72] | 0.54 | 3912/2590 | 1.38 | 9.8 | 52.7 | 1.68; 10 wt % (77 K, 1; 70 bar) |
| SNU-6 (HOHMIB)[72] | 0.54 | 3790/2910$^L$ | 1.51 | 9.7 | 52.2 | 1.68; 10.0 wt % (77 K, 1 atm, 70 bar) |
| UMCM-152 (ANUGIA)[73] | 0.57 | 3726 | 1.34 | 9.4 | 53.2 | 5.7 wt % max excess (77 K) |
| SUKYIH[67] | 0.63 | 3809/1560 | 1.14 | 9.3 | 58.7 | 1.42 wt % (77 K, 1 bar) |
| MOF-505 (RUVKAV)[74] | 0.60 | 3644/3110$^L$ | 1.27 | 9.1 | 54.8 | 4.60;4.82 wt %; 41;43 g/L (77 K, 17; 38 bar) |
| PCN-6[4] | 0.58 | 3592/3800 | 1.26 | 9.0 | 52.4 | 1.9 excess wt% (77K, 1 bar) |
| MOF-5 (SAHYOQ01−05)[4] | 0.590 | 3656/3800 | 1.31 | 8.9 | 54.1 | 7.1 wt % (77 K, 40 bar) |
| MOF-5 Inter (HIFTOG01)[4] | 0.63 | 3434/1130$^L$ | 1.23 | 8.6 | 54.0 | 2.0 wt %; 23.3 g/L (77 K, 1 bar) |
| UMCM-154 (ANUGUM)[73] | 0.68 | 3452 | 1.02 | 8.4 | 57.3 | 5.8 wt % max excess (77 K) |
| MFU-4L (UPOZAB)[75] | 0.56 | 3184/2750 | 1.41 | 8.3 | 46.5 | 4 wt % excess (77 K, 20 bar) |
| NJU-Bai2 (OLOGEC)[76] | 0.59 | 3299/549 | 1.19 | 8.3 | 49.4 | 1.9 wt % (77 K, 20 bar) |
| PCN-46 (LUYHAP)[77] | 0.66 | 3351/2500 | 1.08 | 8.3 | 54.9 | 7.2 wt % (77 K, 60 bar) |
| SNU-15 (COZMUA)[78] | 0.64 | 3315/356 | 1.09 | 8.2 | 52.4 | 0.74 wt % (77 K, 1 bar) |
| IRMOF-9[4] | 0.66 | 3326/1904 | 1.06 | 8.2 | 53.9 | 1.17 excess wt % (77 K, 1 bar) |
| UMCM-150 (OKABAE)[79] | 0.65 | 3126/2980 | 1.16 | 7.9 | 51.3 | 2.2; 5.0 wt % (77 K, 1; 30 bar) |
| FUNBEW[80] | 0.67 | 3179 | 1.05 | 7.9 | 52.8 | 1.6 wt % (77 K, 20 bar) |
| NOTT-140 (EPISOM)[81] | 0.68 | 3132/2620 | 1.05 | 7.8 | 52.7 | 6 wt % (77 K, 20 bar) |
| HKUST-1[5] | 0.89 | 2100/1944 | 0.78 | 4.5 | 39.9 | 3.3 excess wt %; 29 g/L (77 K, 77 bar) |
| UiO-66[82] | 1.24 | 936 | 0.42 | 2.4 | 30.3 | 2.4 wt % (77 K, 31 bar) |

$^a$Data are sorted by gravimetric density, and assembled into two groups: (1) compounds for which no H₂ measurements have been reported (top portion of table), and (2) compounds whose H₂ uptake has been previously assessed (bottom portion of table). Data includes common names, CSD index codes, density, surface area (S.A.), porosity, calculated total weight percent (wt %, g of H₂ per g of MOF), and calculated total volumetric capacity (vol. cap.) at 77 K and 35 bar. When possible, calculated surface areas are compared to experimental (exp.) data. BET surface areas are reported unless otherwise noted ("L" is used to identify Langmuir values). For experiments we use the highest reported surface area. When available, experimental uptake data and the conditions at which those measurements were taken, are reported in the far right column. Unless otherwise indicated, experimental data refer to total uptake.
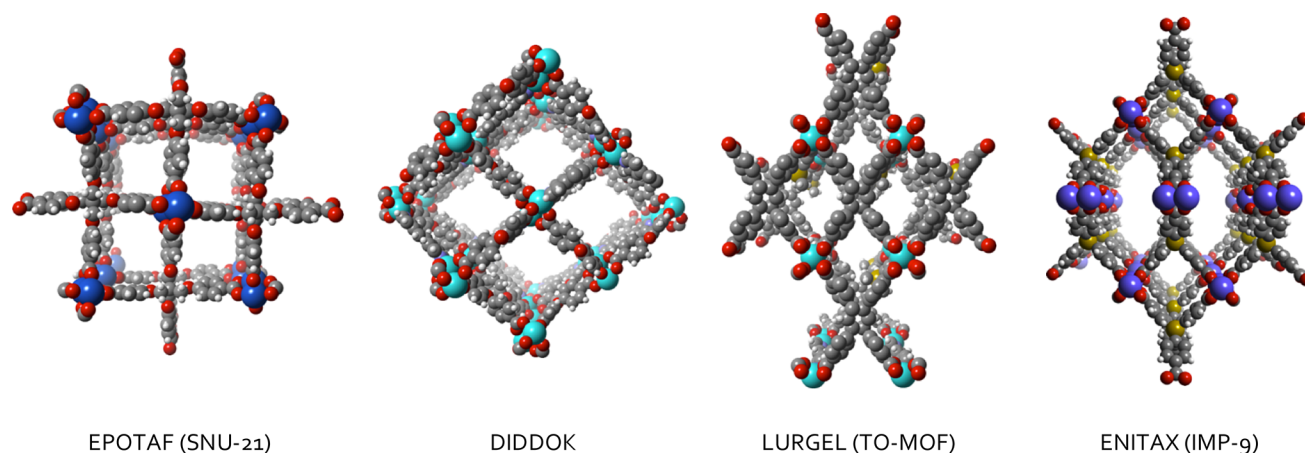


| EPOTAF (SNU-21) | DIDDOK | LURGEL (TO-MOF) | ENITAX (IMP-9) |

**Figure 7.** Crystal structures, CSD identifiers, and MOF names (if known) for four of the top performing MOFs identified by screening.

8−12 wt %, and then decreases for gravimetric densities greater than ∼12 wt %. The decrease in volumetric density at high gravimetric densities is consistent with the density/surface area trade-off suggested in Figure 5, and is similar to what was predicted for CH₄ uptake in MOFs as a function of surface area.[15] We conclude that MOFs having extreme surface areas greater than ∼5500 m²/g cannot meet the DOE volumetric

target (assuming the storage system will have a nonzero volume). Instead, the most promising compounds occur at lower surface areas of 3100−4800 m²/g (Table 1), resulting in both high gravimetric values of 8−12 wt % and volumetric densities of 50−64 g/L. This suggests that development of new MOFs should not exclusively target high surface areas, but

instead focus on achieving moderate mass densities (>0.5 g/$cm^3$) in conjunction with high surface areas.

We now discuss the properties of noteworthy MOFs that emerge from our screening. We begin with MOF-5, which is arguably the most widely studied MOF. As such it serves as a useful benchmark against which we validate our methodology. As previously discussed, optimization of the MOF-5 synthesis protocol has resulted in a continual increase in its surface area, with the highest measured values being similar to those predicted by theory. In addition, MOF-5 is unique in that it is perhaps the only system for which total $H_2$ uptake has been reported on an essentially pristine compound.[29] The measured values of 8.4 wt % and 54.4 g/L (35 bar, 77K) compare very favorably with the 8.9 wt % and 54.1 g/L predicted by our methods. We conclude that our screening approach yields reliable predictions of total $H_2$ uptake.

Turning now to less common compounds, the MOF identified as having the highest theoretical performance is SNU-21, Figure 7.[33] This compound is projected to achieve 12.4 wt % and 71.4 g/L. It has a moderately high theoretical surface area of 5208, yet maintains a mass density of 0.58 g/$cm^3$. The desolvated versions of this compound, SNU-21H and SNU-21S, have had their surface area and hydrogen uptake properties measured experientially, but the reported values (695 (21H) and 905 (21S) $m^2$/g, ~5 wt % total at 77 K and 70 bar;[33] Table 1) fall far below the theoretical expectations. Given that the measured surface area is much less than the theoretical one, it is possible that: some solvent has been retained in the pores, pore-collapse has occurred, the structure is (partially) interpenetrated or has degraded in some way. Therefore, further gains in performance could be realized if the synthesis of a pristine compound could be achieved.

In addition to showing the theoretical performance for well-studied compounds, our screening revealed that there are many "understudied" or "overlooked" MOFs: that is, many MOFs have been synthesized, yet relatively few have had their gas adsorption properties measured. Within this subset of MOFs there exist some with potentially exceptional gas storage properties. These compounds are assembled in the top half of Table 1. For example, Figure 6 identifies CMOF-L4[34] as having the highest theoretical gravimetric uptake overall at greater than 19 wt %. Nevertheless, there appear to be no reported measurements of its hydrogen adsorption properties. Consistent with its high gravimetric $H_2$ density, this MOF is predicted to have the highest overall surface area, ~6400 $m^2$/g, which exceeds that of PCN-610/NU-100[35,36] on a theoretical basis. Despite these exceptional properties, the low density (0.17−0.18 g/L) of CMOF-L4 results in a mediocre volumetric density (~34 g/L) that falls below the DOE target.

The absence of hydrogen uptake measurements in CMOF-L4 could potentially be explained by its unstable structure: the pores in this MOF were found to collapse upon removal of guest molecules.[33] Consequently, we expect that the surface area and $H_2$ capacity of the experimentally realized compound should be much lower than the theoretical prediction. The probability for structure collapse appears to increase as the surface area increases, suggesting that important avenues for MOF research are realizing/stabilizing structures susceptible to collapse, or at least predicting which structures can be realized in pristine, solvent-free form.

Finally, our screening also uncovers several other promising compounds for which no $H_2$ uptake measurements have been reported. They include (using their CSD identifiers): DIDDOK,[37] ENITAX (IMP-9),[38] and LURGEL (TO-MOF).[39] The crystal structures for these MOFs are illustrated in Figure 7. Their positions in the total uptake plot (Figure 6) are indicated with green dashed circles, and it can be seen that they fall near the maximum of the data distribution. Table 1 summarizes their properties; their common features include relatively high mass densities (0.53−0.57 g/$cm^3$), high (but not extreme) surface areas (4162−4651 $m^2$/g), gravimetric densities of 10.2−11.4 wt %, and high volumetric densities of ~60 g/L. All of these compounds appear to have stable structures (i.e., do not exhibit pore collapse upon solvent removal). Because these MOFs have received only minimal experimental scrutiny, they represent targets of opportunity for more extensive synthesis and testing.

## 4. CONCLUSIONS

We have demonstrated an efficient, automated approach for screening the 600 000+ entry Cambridge Structure Database for porous, metal−organic compounds (i.e., MOFs) useful for hydrogen storage. Our approach employs routines for virtual solvent removal, and leverages the established empirical correlation between excess hydrogen uptake and surface area. Consequently, the method is highly efficient since it does not require the evaluation of interatomic potentials or expensive isotherm simulations. Excluding compounds with disorder or missing atoms, we have assembled a database of more than 4000 solvent-free structures for which we assess porosity, surface area, and total theoretical $H_2$ uptake (gravimetric and volumetric). Because our approach relies only on known compounds, it may present advantages to those based on hypothetical compounds that may prove difficult to synthesize.

Analysis of the relationship between MOF mass density and surface area reveals that density decreases with increasing surface area, indicating that a trade-off exists between gravimetric and volumetric $H_2$ storage. The concave downward shape of the volumetric vs. gravimetric uptake distribution further supports this conclusion: volumetric $H_2$ density reaches a maximum for surface areas in the range of 3100−4800 $m^2$/g, but then decreases for those compounds having larger surface areas. The data suggests that development of new MOFs should not exclusively target high surface areas, but instead focus on achieving moderate mass densities (>0.5 g/$cm^3$) in conjunction with high surface areas.

Our screening identifies several compounds with promising properties. While some of these have had their experimental $H_2$ uptake tested, many appear to have undergone no testing whatsoever. Of these, SNU-21 emerges at the highest-performing candidate, achieving densities of 12.4 wt % and 71.4 g/L. However, experimental measurements on this compound have not achieved these high levels of performance, presumably due to incomplete solvent removal. In addition, the compounds having CSD identifiers (common names) DIDDOK, ENITAX (IMP-9), and LURGEL (TO-MOF) are highlighted as "targets of opportunity" given their high $H_2$ densities (10.0−11.4 wt % and ~60 g/L) and absence of uptake measurements.

Looking to the future, we suggest that research efforts targeting MOFs for gas storage emphasize the challenges of structure stability/pore collapse and solvent removal. Many promising compounds in our data set exhibit these deficiencies, and we believe these issues warrant additional effort to quantify the factors that determine whether a given compound can be realized in a robust, solvent-free form.

H

dx.doi.org/10.1021/cm401978e | *Chem. Mater.* XXXX, XXX, XXX−XXX

## ■ ASSOCIATED CONTENT

**S** Supporting Information

Atomic number density of database MOFs versus surface area; MOF-5 surface area vs publication year; histograms of pore volume and void %. This material is available free of charge via the Internet at http://pubs.acs.org.

## ■ AUTHOR INFORMATION

**Corresponding Author**
*E-mail: djsiege@umich.edu.

**Notes**

The authors declare no competing financial interest.

## ■ ACKNOWLEDGMENTS

## ■ REFERENCES

(1) Chu, S.; Majumdar, A. *Nature* **2012**, *488*, 294.
(2) Yang, J.; Sudik, A.; Wolverton, C.; Siegel, D. J. *Chem. Soc. Rev.* **2010**, *39*, 656.
(3) Sculley, J.; Yuan, D.; Zhou, H.-C. *Energy Environ. Sci.* **2011**, *4*, 2721.
(4) Suh, M. P.; Park, H. J.; Prasad, T. K.; Lim, D. W. *Chem. Rev.* **2012**, *112*, 782.
(5) Murray, L. J.; Dinca, M.; Long, J. R. *Chem. Soc. Rev.* **2009**, *38*, 1294.
(6) Ferey, G. *Chem. Soc. Rev.* **2008**, *37*, 191.
(7) Rowsell, J. L. C. Y.; O., M. *Microporous Mesoporous Mater.* **2004**, *73*, 3.
(8) Batten, S. R. N., S. M.; Turner, D. R. *Coordination Polymers: Design, Synthesis, and Application*; Royal Society of Chemistry: Cambridge, U.K., 2009.
(9) *Design and Construction of Coordination Polymers*; Hong, M.-C. C., L., Ed.; John Wiley & Sons: Hoboken, NJ, 2009.
(10) Li, J.-R.; Kuppler, R. J.; Zhou, H.-C. *Chem. Soc. Rev.* **2009**, *38*, 1477.
(11) Meek, S. T.; Greathouse, J. A.; Allendorf, M. D. *Adv. Mater.* **2011**, *23*, 249.
(12) Koh, H. S.; Rana, M. K.; Hwang, J.; Siegel, D. J. *Phys. Chem. Chem. Phys.* **2013**, *15*, 4573.
(13) Caskey, S. R.; Wong-Foy, A. G.; Matzger, A. J. *J. Am. Chem. Soc.* **2008**, *130*, 10870.
(14) Ockwig, N. W.; Delgado-Friedrichs, O.; O'Keeffe, M.; Yaghi, O. M. *Acc. Chem. Res.* **2005**, *38*, 176.
(15) Wilmer, C. E.; Leaf, M.; Lee, C. Y.; Farha, O. K.; Hauser, B. G.; Hupp, J. T.; Snurr, R. Q. *Nat Chem* **2012**, *4*, 83.
(16) Allen, F. H. *Acta Crystallogr., Sect. B* **2002**, *58*, 380.
(17) First, E. L.; Floudas, C. A. *Microporous Mesoporous Mater.* **2013**, *165*, 32.
(18) Haldoupis, E.; Nair, S.; Sholl, D. S. *Phys. Chem. Chem. Phys.* **2011**, *13*, 5053.
(19) Lin, L.-C.; Berger, A. H.; Martin, R. L.; Kim, J.; Swisher, J. A.; Jariwala, K.; Rycroft, C. H.; Bhown, A. S.; Deem, M. W.; Haranczyk, M.; Smit, B. *Nat. Mater.* **2012**, *11*, 633.
(20) Wilmer, C. E.; Farha, O. K.; Bae, Y.-S.; Hupp, J. T.; Snurr, R. Q. *Energy Environ. Sci.* **2012**, *5*, 9849.
(21) Haldoupis, E.; Nair, S.; Sholl, D. S. *J. Am. Chem. Soc.* **2010**, *132*, 7528.
(22) Watanabe, T.; Sholl, D. S. *Langmuir* **2012**, *28*, 14114.
(23) Düren, T.; Millange, F.; Férey, G.; Walton, K. S.; Snurr, R. Q. *J. Phys. Chem. C* **2007**, *111*, 15350.
(24) Bahn, S. R.; Jacobsen, K. W. *Comput. Sci. Eng.* **2002**, *4*, 56.
(25) Spek, A. L. *J. Appl. Crystallogr.* **2003**, *36*, 7.
(26) Panella, B.; Hirscher, M.; Roth, S. *Carbon* **2005**, *43*, 2209.
(27) Kolotilov, S. V.; Pavlishchuk, V. V. *Theor. Exp. Chem.* **2009**, *45*, 75.
(28) Gross, K. J.; Carrington, K. R.; Barcelo, S.; Karkamkar, A.; Purewal, J.; Ma, S.; Zhou, H.-C.; Dantzer, P.; Ott, K.; Burrell, T.; Semeslberger, T.; Pivak, Y.; Dam, B.; Chandra, D. *Recommended Best Practices for the Characterization of Storage Properties of Hydrogen Storage Materials*; Department of Energy: Washington, D.C., 2012
(29) Kaye, S. S.; D., A.; Yaghi, O. M.; Long, J. R. *J. Am. Chem. Soc.* **2007**, *129*, 14176.
(30) Purewal, J.; Liu, D.; Sudik, A.; Veenstra, M.; Yang, J.; Maurer, S.; Müller, U.; Siegel, D. J. *J. Phys. Chem. C* **2012**, *116*, 20199.
(31) Purewal, J. J.; Liu, D.; Yang, J.; Sudik, A.; Siegel, D. J.; Maurer, S.; Müller, U. *Int. J. Hydrogen Energy* **2012**, *37*, 2723.
(32) Schnobrich, J. K.; Koh, K.; Sura, K. N.; Matzger, A. J. *Langmuir* **2010**, *26*, 5808.
(33) Kim, T. K.; Suh, M. P. *Chem. Commun.* **2011**, *47*, 4258.
(34) Liqing Ma, J. M. F.; Abney, C.; Lin, W. *Nat. Chem.* **2010**, *2*, 838.
(35) Farha, O. K.; Yazadyn, A. O.; Eryazici, I.; Malliakas, C. D.; Hauser, B. G.; Kanatzidis, M. G.; Nguyen, S. T.; Snurr, R. Q.; Hupp, J. T. *Nat. Chem.* **2010**, *2*, 944.
(36) Yuan, D.; Zhao, D.; Sun, D.; Zhou, H.-C. *Angew. Chem., Int. Ed.* **2010**, *49*, 5357.
(37) Kondo, M.; Irie, Y.; Miyazawa, M.; Kawaguchi, H.; Yasue, S.; Maeda, K.; Uchida, F. *J. Organomet. Chem.* **2007**, *692*, 136.
(38) Davies, R. P.; L., R.; Lickiss, P. D.; Robertson, K.; White, J. J. P. *Cryst. Growth Des.* **2010**, *10*, 4571.
(39) Gadzikwa, T.; F., O. K.; Malliakas, C. D.; Kanatzidis, M. G.; Hupp, J. T.; Nguyen, S. T. *J. Am. Chem. Soc.* **2009**, *131*, 13613.
(40) Ma, S.; S., D.; Ambrogio, M.; Fillinger, J. A.; Parkin, S.; Zhou, H.-C. *J. Am. Chem. Soc.* **2007**, *129*, 1858.
(41) Wang, X.-S.; M., S.; Sun, D.; Parkin, S.; Zhou, H.-C. *J. Am. Chem. Soc.* **2006**, *128*, 16474.
(42) Grünker, R.; Senkovska, I.; Biedermann, R.; Klein, N.; Klausch, A.; Baburin, I. A.; Mueller, U.; Kaskel, S. *Eur. J. Inorg. Chem.* **2010**, *2010*, 3835.
(43) Schnobrich, J. K.; Lebel, O.; Cychosz, K. A.; Dailly, A.; Wong-Foy, A. G.; Matzger, A. J. *J. Am. Chem. Soc.* **2010**, *132*, 13941.
(44) Inokuma, Y.; Arai, T.; Fujita, M. *Nat. Chem.* **2010**, *2*, 780.
(45) Liu, T. F.; Lu, J.; Lin, X.; Cao, R. *Chem. Commun.* **2010**, *46*, 8439.
(46) Yanxiong, K.; C., D. J.; Sun, D.; Zhou, H.-C. *Inorg. Chem. Commun.* **2006**, *45*, 1897.
(47) Prior, T. J.; Bradshaw, D.; Teat, S. J.; Rosseinsky, M. J. *Chem. Commun.* **2003**, 500.
(48) Bauer, C. A.; T., T. V.; Settersten, T. B.; Patterson, B. D.; Liu, V. H.; Simmons, B. A.; Allendorf, M. D. *J. Am. Chem. Soc.* **2007**, *129*, 7136.
(49) Wollmann, P.; Leistner, M.; Stoeck, U.; Grunker, R.; Gedrich, K.; Klein, N.; Throl, O.; Grahlert, W.; Senkovska, I.; Dreisbach, F.; Kaskel, S. *Chem. Commun.* **2011**, *47*, 5151.
(50) Schaate, A.; Roy, P.; Godt, A.; Lippke, J.; Waltz, F.; Wiebcke, M.; Behrens, P. *Chemistry* **2011**, *17*, 6643.
(51) Farha, O. K.; M., C. D.; Kanatzidis, M. G.; Hupp, J. T. *J. Am. Chem. Soc.* **2010**, *132*, 950.
(52) Han, Y.; Li, X.; Li, L.; Ma, C.; Shen, Z.; Song, Y.; You, X. *Inorg. Chem.* **2010**, *49*, 10781.
(53) Mei-Jin Lin, A. J.; Kyritsakas, N.; Hosseini, M. W. *CrystEngComm* **2009**, *11*, 189.
(54) Choi, E.-Y.; B., P. M.; Novotny, R. W.; Son, H.-T.; Hu, C.; Choe, W. *Inorg. Chem. Commun.* **2009**, *48*, 426.
(55) Nelson, A. P.; F., O. K.; Mulfort, K. L.; Hupp, J. T. *J. Am. Chem. Soc.* **2009**, 131.
(56) Haneul Yim, E. K.; Kim, J. *Bull. Kor. Chem. Soc.* **2010**, *31*, 1041.
(57) Li, Y.; Song, D. *CrystEngComm* **2011**, *13*, 1821.
(58) Biradha, K.; Fujita, M. *Chem. Commun.* **2001**, *0*, 15.

(59) Norberto Masciocchi, S. G.; Colombo, V.; Maspero, A.; Palmisano, G.; Seyyedi, B.; Lamberti, C.; Silvia, B. *J. Am. Chem. Soc.* **2010**, *132*, 7902.

(60) Park, H. J.; Cheon, Y. E.; Suh, M. P. *Chemistry* **2010**, *16*, 11662.

(61) Stergiannakos, T.; Tylianakis, E.; Klontzas, E.; Froudakis, G. E. *J. Phys. Chem. C* **2010**, *114*, 16855.

(62) Shuting, W.; M., L.; Long, L.-S.; Zheng, L.-S.; Lin, W. *Inorg. Chem.* **2009**, *48*, 2436.

(63) Eddaoudi, M.; Kim, J.; Rosi, N.; Vodak, D.; Wachter, J.; O'Keeffe, M.; Yaghi, O. M. *Science* **2002**, *295*, 469.

(64) Sun, D.; Ke, Y.; Mattox, T. M.; Ooro, B. A.; Zhou, H. C. *Chem Commun* **2005**, 5447.

(65) Sumida, K.; H., M. R.; Horike, S.; Dailly, A.; Long, J. R. *J. Am. Chem. Soc.* **2009**, *131*, 15120.

(66) Grunker, R.; Senkovska, I.; Biedermann, R.; Klein, N.; Lohe, M. R.; Muller, P.; Kaskel, S. *Chem. Commun.* **2011**, *47*, 490.

(67) Ma, L.; Jin, A.; Xie, Z.; Lin, W. *Angew. Chem., Int. Ed.* **2009**, *48*, 9905.

(68) Wang, X. S.; Ma, S.; Yuan, D.; Yoon, J. W.; Hwang, Y. K.; Chang, J. S.; Wang, X.; Jorgensen, M. R.; Chen, Y. S.; Zhou, H. C. *Inorg. Chem.* **2009**, *48*, 7519.

(69) Koh, K.; Van Oosterhout, J. D.; Roy, S.; Wong-Foy, A. G.; Matzger, A. J. *Chemical Science* **2012**, *3*, 2429.

(70) Sun, D.; Collins, D. J.; Ke, Y.; Zuo, J. L.; Zhou, H. C. *Chemistry* **2006**, *12*, 3768.

(71) Song, X.; Zou, Y.; Liu, X.; Oh, M.; Lah, M. S. *New J. Chem.* **2010**, *34*, 2396.

(72) Park, H. J.; Suh, M. P. *Chemistry* **2008**, *14*, 8812.

(73) Schnobrich, J. K.; L., O.; Cychosz, K. A.; Dailly, A.; Wong-Foy, A. G.; Matzger, A. J. *J. Am. Chem. Soc.* **2010**, *132*, 13941.

(74) Zheng, B.; Liang, Z.; Li, G.; Huo, Q.; Liu, Y. *Cryst. Growth Des.* **2010**, *10*, 3405.

(75) Denysenko, D.; Grzywa, M.; Tonigold, M.; Streppel, B.; Krkljus, I.; Hirscher, M.; Mugnaioli, E.; Kolb, U.; Hanss, J.; Volkmer, D. *Chem.—Eur. J.* **2011**, *17*, 1837.

(76) Duan, J.; Bai, J.; Zheng, B.; Li, Y.; Ren, W. *Chem. Commun.* **2011**, *47*, 2556.

(77) Zhao, D.; Yuan, D.; Yakovenko, A.; Zhou, H. C. *Chem. Commun.* **2010**, *46*, 4196.

(78) Cheon, Y. E.; Suh, M. P. *Chem. Commun.* **2009**, 2296.

(79) Park, T. H.; Cychosz, K. A.; Wong-Foy, A. G.; Dailly, A.; Matzger, A. J. *Chem. Commun.* **2011**, *47*, 1452.

(80) Liu, B.; Sun, C.; Chen, G. *Chem. Eng. Sci.* **2011**, *66*, 3012.

(81) Tan, C.; Yang, S.; Champness, N. R.; Lin, X.; Blake, A. J.; Lewis, W.; Schroder, M. *Chem. Commun.* **2011**, *47*, 4487.

(82) Chavan, S.; Vitillo, J. G.; Gianolio, D.; Zavorotynska, O.; Civalleri, B.; Jakobsen, S.; Nilsen, M. H.; Valenzano, L.; Lamberti, C.; Lillerud, K. P.; Bordiga, S. *Phys. Chem. Chem. Phys.* **2012**, *14*, 1614.